



Contents lists available at CEPM

Computational Engineering and Physical Modeling

Journal homepage: www.jcepm.com

Dynamic and Fatigue Life Prediction Analysis of Airfield Runway Rigid Pavement Using Finite Element Method

K. Kavin Mathi¹, K. Nallasivam^{2*} 

1. PG Student of Transportation Engineering, Department of Civil Engineering, National Institute of Technology (NIT) Hamirpur, Himachal Pradesh, India
2. Assistant Professor of Department of Civil Engineering, National Institute of Technology (NIT) Hamirpur 177001, Himachal Pradesh, India

Corresponding author: nallasivam@nith.ac.in

 <https://doi.org/10.22115/CEPM.2022.347999.1215>

ARTICLE INFO

Article history:

Received: 21 June 2022

Revised: 11 August 2022

Accepted: 29 October 2022

Keywords:

Airfield runway rigid pavement;

FEM;

Dynamic analysis;

Fatigue life prediction.

ABSTRACT

The significance of rigid airfield pavements is growing as airline travel becomes more sophisticated. Apart from the geometrics of runway design, an efficient runway should satisfy structural aspects. In this connection, greater emphasis should be placed on pavement slab analysis and design. The research analyzes the dynamic analysis of a 3-dimensionally formed concrete slab resting on a subgrade foundation, which is a homogeneous, isotropic elastic half-space model, in order to assess the performance of variation in Young's modulus in compared to Winkler's reaction modulus. The influence and impact of two distinct landing gear configurations, especially tridem and tandem-dual wheels of the A-380 and A-310, on varying slab structural parameters such as concrete's modulus of elasticity, slab thickness, and temperature gradients are explored. The aircraft load stresses are evaluated using the finite element programme ANSYS APDL 2021R2 version, which models the slab as a 3-D element with an 8-noded-solid 185 element type. The above-mentioned pavement models' modal and dynamic (transient) analyses were performed for different take-off speeds, and a comparison is conducted for the present standard strength and high strength concrete types. Miner's rule and the Rainflow counting technique are used to estimate the fatigue life based on the findings of the transient analysis. The fatigue life for high-strength concrete is found to be 50% more. The fatigue life is 36% higher for the A-380 load, indicating that a material's fatigue property is entirely determined by its load frequency rather than its magnitude.

How to cite this article: Mathi KK, Nallasivam K. Dynamic and fatigue life prediction analysis of airfield runway rigid pavement using finite element method. *Comput Eng Phys Model* 2022;5:1–23. <https://doi.org/10.22115/cepm.2022.347999.1215>

2588-6959/ © 2022 The Authors. Published by Pouyan Press.

This is an open access article under the CC BY license (<http://creativecommons.org/licenses/by/4.0/>).



1. Introduction

When it concerns the establishment and economic development of the country, one of the industries that make the most significant contribution is the transportation industry. The need for airports that are measured to international standards has increased all around the world. These heavy weights—new generation aircraft having different landing gear configurations—have also posed several challenges to civil engineers as they mainly affect the existing methods of airport pavement design. The dynamic interaction between the aircraft and the rigid pavement is taken into consideration in the modelling technique. The rigid pavement is modeled as a series of thin-plate finite components that are held together by a viscoelastic foundation. The numerical results of the proposed analytical formulation are compared to previous analytical solutions and experimental data [1]. Using a finite element-based dynamic analysis technique, the response of rigid airport pavements with Viscoelastic subgrade to a moving aircraft simulated by the spring and dashpot suspensions and a temperature gradient across the depth is explored [2]. The dynamic vehicle-pavement-foundation interaction effects are taken into consideration using the 3D finite-element technique. It is taken into consideration how concrete pavements interact with the underlying soil foundation. A study [3] looked at the effects of several parameters on the dynamic response of concrete pavements subjected to moving loads. The similarities between the well-known Winkler foundation response and parametric research are done to explore some essential features of the dynamic behaviour of rigid concrete pavements utilising a Finite Element formulation of a thick plate on an elastic foundation. The dynamic behaviour of stiff concrete pavements is studied using parametric analyses based on a Finite Element formulation of a thick plate on an elastic basis. The parametric experiments examine the impacts of structural damping, vehicle speed, and soil stiffness on the response of concrete pavements to single-wheel and HS20 loads, as well as the distinction between static and dynamic response. Wheels are moved over the pavement's edge and centerline, and a dynamic time domain analysis is used to determine the consequent deflections and major tensile stresses. The numerical analysis' findings suggest that the Winkler soil model may drastically overdesign the pavement by overestimating structural reactions. The relevance of dynamic analysis is shown to be important, as are the impacts of structural damping and soil stiffness. However, this research finds that the impact of vehicle speed is comparatively less important [4]. The behaviour of concrete pavements under dynamic loads has received much less study than the behaviour of concrete pavements under static loads. A 3D finite element analysis was performed using multiple axle groups at various critical speeds and dynamic amplification, as well as the critical location of fatigue cracking [2]. The response of dowel jointed concrete pavements to the combined effects of nonlinear temperature gradient and moving axle load is evaluated using 3D finite element modelling [5]. To analyse rigid pavements exposed to moving traffic or aircraft loads, the revised solution technique uses a finite-element approach. The concrete pavement is discretized using thick plate components, which account for transverse shear deformation and bending. To simulate the underlying soil media, elastic spring and dashpot devices are employed. The dynamic interaction between the moving load and the pavement is taken into consideration by modelling the vehicle using a spring–dashpot unit [6]. The dynamic response of an infinite plate resting on an elastic foundation exposed to moving traffic load with changing velocity is studied using a triple Fourier integral transform in time and space.

Initial velocity, acceleration, and deceleration are the most important affecting parameters [7]. The dynamic analysis of rigid pavements exposed to moving loads, including vehicle–pavement interaction, is detailed, with the underlying soil medium being simulated using the Pasternak model. A thorough investigation of the range of velocities for finite and infinite length pavements resting on a two-parameter soil medium was carried out. [8] The effects of soil modulus, shear modulus, pavement thickness, and vehicle–pavement interaction on pavement response were studied. A MATLAB programme and a FEM ABAQUS model are used to predict the dynamic behaviour of airport concrete pavements under aircraft impact loads [9]. When building pavement that will be subjected to repetitive action of moving loads, fatigue behaviour is also a significant aspect to consider. The repeated action of transferring load on the airport pavement may result in fatigue cracks and, in severe cases, runway pavement component failure. Studies on fatigue behaviour were conducted, and the analytical and experimental findings were found to be quite consistent [10]. The applicability of Miner's Hypothesis to specific concrete specimen fatigue failure has also been thoroughly examined using slab fatigue tests and accelerated pavement testing (APT) under cyclic loads. The fatigue life of concrete slabs is substantially longer than that of beams, according to laboratory tests, with the increase in fatigue life dependent on slab shape, thickness, loading configuration, concrete composition, and boundary conditions [11]. The study used 22 beams based on the Timoshenko beam concept to predict fatigue life due to moving loads. The dynamic response of continuous beams was found to be equal to the static response, resulting in a dynamic amplification factor of 1.1 [12]. Vehicle axle dynamic loads deviate from static loads because pavement surfaces are not perfectly level. More dynamic loads cause pavement deterioration to occur more quickly. The evenness of the pavement also declines as it loses quality, and the IRI roughness rating rises. The maximal dynamic loads rise, as does their damaging impact on the pavement's structural integrity. This research is to evaluate how pavement distress is impacted by dynamic stresses brought on by pavement roughness. Therefore, reduced initial pavement roughness brought about by high-quality road construction and appropriate maintenance of the pavement while it is in use will lessen pavement distress and lengthen its useful life [13]. On the basis of a unified analytical framework, the dynamic response of a pavement structure to a moving vehicle load is examined. By combining the traits of a road profile, a moving vehicle, and a slab on a viscoelastic foundation, the time-dependent deflection and its resulting dynamic quantities for a slab construction are achieved. A rigid pavement structure's dynamic deflection and dynamic stresses may be understood numerically using the model. It has been discovered that the impact of surface roughness on a slab structure's dynamic response has a significant impact on the useful life of the structure and may be taken into consideration when designing a pavement. In order to evaluate the subgrade support for a pavement as it matures, the model may be calibrated to determine the k-value [14]. To predict viscoelastic pavement responses under moving loads and irregular tyre contact stresses, the research uses the finite element method (FEM). Asphalt pavements with four different asphalt layer thicknesses were studied to determine the effects of loading pattern and speed on pavement surface deflection and strain responses. Surface deflections, maximum tensile stresses in the asphalt layer, and maximum compressive strains on top of the subgrade were among the pavement reactions that were examined. The study's findings suggest that the suggested FEM can quickly compute asphalt pavement reactions to moving loads for mechanistic-empirical pavement design and analysis [15]. In the mechanistic–empirical design

of airport pavement, the fatigue model is critical. The fatigue model for cement concrete pavement shows how stress and the number of load repetitions are related. Full-scale testing-based fatigue models and concrete beam testing-based fatigue models are the two forms of fatigue models. The regression analysis procedure and stress calculation approach for each fatigue model were then described [16]. The runway must be built to withstand the heavy wheel weight of the aircrafts the airport will be serving in order to achieve flight safety regulations. The Federal Aviation Administration's (FAA) technique and the COMFAA software have been used in the research to assess the thickness and strength of the runway pavement. Based on the layout of the landing wheels, the Boeing 747-400ER was utilized as the reference aircraft. If the PCN value is greater than the ACN value, the pavement structure is capable of supporting the weight of all aircraft types that are intended to use the runway [17]. Pavement thickness design and pavement life prediction are two separate concepts, as shown by a case study on a rigid aircraft pavement. By using Monte Carlo modelling, it was determined that 98.5 % of the pavement as it was built was stronger than the pavement that had been intended for it, and that the pavement's estimated fatigue life was around 180 times longer than the useful design life. The practical observation that rigid aircraft pavement service life often surpasses normal structural design lifetimes was explained by the large discrepancy between pavement design and pavement life forecast, it was determined [18]. It has been observed that a large number of closed form and non-closed form: finite elements, Finite difference method were developed by different researchers for the analysis of pavement. While a few of them were not completely robust in the representation of all the complex actions of a pavement, the 8 noded shell element with six degrees of freedom at each node was observed to be very well representative of the structural actions and computationally efficient. While some researcher carried out free vibration analysis based on closed form solution, a few conducted finite element analysis. Since natural frequencies are important parameters to be considered in design, especially for checking the safety of pavement under dynamic excitation, use of appropriate finite element formulation is necessary to accurately predict the same. Airfield Pavements are susceptible to repetitive airfield moving vehicular loads, which may develop fatigue crack and sometimes lead to the failure of a component of a pavement. Fatigue behavior is also an important consideration for the design of pavement subjected to repeated action of moving airfield loads. An airfield vehicle passage over a pavement induces loads, which vary with the time leading to the development of fatigue in the structural member. The fatigue provisions in the codes of practice for the design of pavement do not explicitly consider the stresses induced in the pavement components due to dynamic interaction with the moving airfield vehicles. Literature survey shows that Fatigue behaviour of pavement structures has been studied by fewer authors theoretically as well as experimentally. The present study has been undertaken to evaluate the fatigue damage of airfield pavement from airline vehicle induced stress history by using time domain method.

2. Research significance

The study focuses on proposing structurally adequate concrete pavement for the proposed Airfield runway with heavy aircrafts by carrying out finite element modelling using dynamic analysis and fatigue life prediction. To achieve the above objectives, the scope of work is:

- To perform modal and dynamic analysis using FEM and show the stress-time history.

- To determine the fatigue life and to find its structural capability in terms of damage index.

3. Study areas

The approach is applied to Mangalore International Airport in Karnataka (Fig.1), India, to enable broad body aircraft such as the A- 370and A- 380. The asphalt and concrete runways are 1,615m and 2,450m long, respectively, with magnetic azimuths of 09/27 and 06/24.



Fig .1. Map of Mangalore airport showing the existing runways and proposed extension runway.

4. FEM modeling of airfield pavement by ANSYS

4.1. Element properties and material mechanical characteristics of layer forming in rigid pavement

The rigid pavement consists of cement concrete slab, sub base and subgrade. For each concrete slab model all the 3 layers are finite element meshing is done The pavement modeled by finite element software ANSYS APDL 2021R2 version, which models slab as a 3-D element with 8 noded -solid 185 element type.

Table 1

Mechanical Characteristics Input Parameters of layer forming in Rigid pavement.

Layer	Elastic modulus (E) MPa	Poisson's ratio(μ)	Layer Density(γ)	Element Type
Concrete slab	25000, 30000, 40000, 50000	0.15	2.40E-03	8 noded - solid 185
Sub base	144.158	0.3	6.00E-04	8 noded - solid 185
Subgrade	17.1616	0.4	3.00E-04	8 noded - solid 185

Four concrete types having their modulus of elasticity i.e., 25000MPa, 30000MPa, 40000MPa, 50000MPa as described in Table 1 are taken and a Poisson's ratio value of 0.15 is considered.

4.2. Aircraft loading scheme and static analysis using finite element method -ANSYS

An elastic half-space was assumed as foundation so that the influence of the variation of Young's modulus was examined in contrast with Winkler's reaction modulus. Different gear locations of A-310 and A-380 aircrafts were evaluated. The computation model consists of the 3D homogeneous, isotropic rectangular shaped slabs concrete slab model uniformly resting on sub-base and foundation layer. Evaluation of stresses due to A-380 having TRDT landing gear configuration is done. It is compared with that of A-310's TADT landing gear configuration. The Airbus A-380 has the biggest take-off weight as well as the most complex landing gear. The influence of each landing gear is taken separately due to the larger distance between the landing gears. The gross take-off weight from A-310 and A-380 that are transmitted through TADT and TRDT landing gears are $P = 67500 \text{ kg}$, $P = 165000 \text{ kg}$. Based on the tyre imprint loading as mentioned in the calculation below, the equivalent rectangular area of wheel loading is found out for corresponding tyre pressures of A-310 and A-380. These wheel loads are applied on the nodal points giving due regard to the spacing between the axles and wheel spacing. The temperature gradient (linear) values were introduced to the ANSYS model at the top and bottom surface of the slab. The meshing is done in three layers for better accuracy of results.

4.2.1. Slab loading positions

The landing gear-loading position on the concrete slab is taken into consideration in order to obtain the most disadvantageous bending tensile stress values. Simulations are performed, in different loading positions, such as: D1-centre of slab, D2- tangential to the length of the slab(Fig .2), D3-at the corner of the slab(Fig. 3), and D4(Fig.4), - tangential to the contraction-expansion joint. The aircraft weight is transmitted to the concrete slab in the form of uniformly distributed loads in a quasi-elliptical area. It is concluded that the D2 loading position generates the highest bending tensile stress values. It requires higher calculating time so an equivalent rectangular loading area having tire imprint of length L_e is chosen. Fig.14 shows the flowchart (Appendix-A)

4.2.2. Loading area of tyre imprint

The equivalent rectangular tyre imprint area $= 0.5227 L_e^2$

Length of rectangular area $= 0.8172(L_e)$

Width rectangular area $= 0.6 L_e$

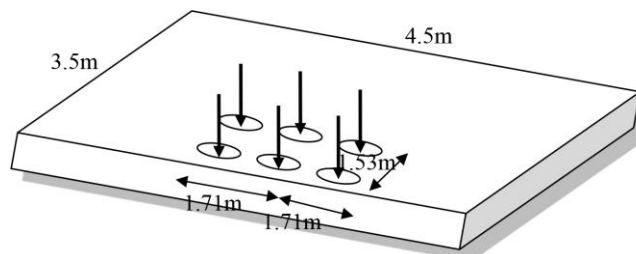


Fig. 2. Airbus 310 - Landing Gear in D2 Loading Position

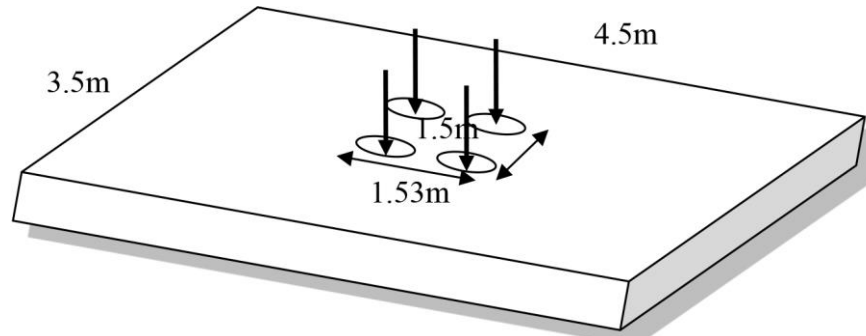


Fig. 3. Airbus 310 - Landing Gear in D3 Loading Position

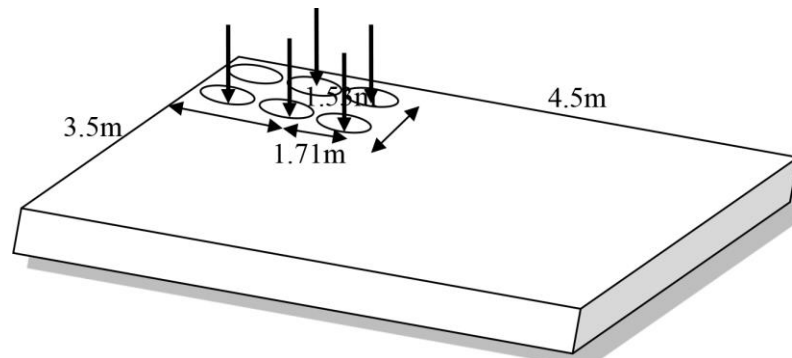


Fig. 4. Airbus 310 - Landing Gear in D4 Loading Position

4.2.3. Determination of tyre contact area for a given landing gear configuration

1. for Airbus–310:

tyre pressure	=	12 kg/cm ²
Load on one landing gear	=	67.88 tonne load
Load on 1 tyre	=	16970 kg
tyre imprint area	=	1414.167 cm ²
$0.5227L^2$	=	1414.167
L^2	=	2705.503
L	=	52.01445 cm
$0.6L$	=	31 cm
$0.8712L$	=	45 cm

2. for Airbus–380:

tyre pressure	=	15kg/cm ²
Load on one landing gear	=	165 tonne load
Load on 1 tyre	=	41250 kg
tyre imprint area	=	3437.5 cm ²
$0.5227L^2$	=	3437.5
L	=	81.09cm
$0.6L$	=	49 cm
$0.8712L$	=	71 cm

Thus for A-310's and A-380's landing gear configuration, a tyre imprint area of 31 cm x 45 cm and 49 cm x 71 cm are obtained.

5. Modal analysis

The studies on free vibrational characteristics of airfield pavement have been carried out since the modal parameters like natural frequencies and mode shapes are important for understanding the dynamic behavior of the airfield pavement structure. The airfield pavement systems with continuously distributed mass have infinite number of natural frequencies, however, only few lower of those frequencies have practical significance. The natural frequencies and mode shape obtained from the theoretical FEM analysis. The subsequent studies on complex dynamic analysis and fatigue analysis due moving airfield vehicle have been carried out based on the satisfactory performance of the evaluated modal parameters.

5.1. Eigen value problem for un-damped system

The general equation of motion for an un-damped free vibration system can be written as

$$[M][\ddot{\delta}] + [K][\delta] = 0 \quad (1)$$

where $[\delta]$, $[\ddot{\delta}]$ are the values of the global displacements and accelerations,

$[K]$ and $[M]$ are the global stiffness and mass matrix after applying boundary conditions.

Assuming harmonic motion in natural mode of vibration, the response can be written as

$$\{\delta\} = \{X\} \sin(\omega t + \phi) \quad (2)$$

where $\{X\}$ is the vector of nodal amplitude of vibration, ω is the circular natural frequency of vibration [rad/sec] and ϕ is the phase angle.

Substitution of (2) in (1) leads to the generalized eigen value problem.

$$\{ [K] - \omega^2 [M] \} \{ X \} = 0 \quad (3)$$

Eq. (3) is solved using a standard eigen solver to obtain the values of natural frequencies and mode shapes of the pavement.

6. Dynamic analysis of the proposed pavement

Dynamic analysis is concerned with treating the load as a time-varying or space-varying entity. The configuration, amplitude, frequency, and location of applied loads influence the structural dynamic response of the pavement.

6.1. Stresses-time history curves from transient analysis

The transient dynamic analysis for wheel loads is carried out by varying the location of wheel load along the pavement edge as this case yields the maximum stress built in the concrete slab. The transient dynamic analysis is done over for pavement thicknesses of 20 cm, 25 cm, 30 cm, 35 cm, and 40 cm by moving the TRDT and TADT landing gear configuration of A-310 and A-380 for

design take-off speeds of 160 kmph and 260 kmph. The majority of commercial airplanes really take off at around the same speed. The takeoff speed of an A380 is around 260 kmph, whereas that of an A310 is approximately 160 kmph. The precise takeoff speed depends on how much cargo and people are being carried. You consider an A310 to be traveling at a higher speed than an A380 during takeoff, however, this is an optical illusion brought on by the aircraft being in the air and the A380 being considerably longer than an A310. Because aircraft operate practically out of thin air, there are no in-plane reference items for your eyes to accurately estimate the speed. Instead, your eyes only sense velocity in relation to other things moving in the same plane as the aircraft. In the case mentioned above, the aircraft itself is the only point of reference remaining, and your perception of the aircraft's speed will depend on how quickly it travels in relation to its own length. Due to the fact that an A380 is twice as long as an A310, even if they are both travelling at the same speed, the A310 travels more quickly compared to its length than the A380, giving the impression that the A320 is travelling more quickly than it really is.

The comparison study is effected between the two concrete material types belonging to conventional or standard strength and high strength concrete. Ramped loading condition is taken in the case of transient effects. The final analysis is done using large transient displacement. The time step is given at the completion of each load step based on modal analysis. The number of sub-steps is taken to be 10, which gives the segmentation for the stress-time history curve. The final output is the stress-time history graphs for specified node which shows the time in seconds and stress in kg/cm^2 along the x and y axis respectively.

7. Fatigue life prediction analysis

Structures subjected to repeated variable loads may fail in fatigue at stress levels much lower than those required to cause failure under static circumstances. Fatigue failure is described as the accumulation of localised irreversible damage in a structure subjected to time-dependent loads and stresses, and it may have an impact on design. With each load cycle, the amount of damage increases. This kind of damage is cumulative, meaning that it continues to build up until the system fails. If fatigue cracks are discovered early enough, they may be repaired. One example of a similar scenario that may exist is the pavement. The method for calculating the fatigue life of airport runway pavement using vehicle-induced stress history has been described.

7.1. Fatigue strength test

The most fundamental of all fatigue load processes is periodic load, which is defined as a load cycle with constant amplitude. The empirical findings of such constant amplitude studies provide the basis for predicting fatigue life over complex time histories. The stress range, which is defined as the difference between maximum and lowest stress, is found to be strongly dependent on fatigue failure in this situation. A typical stress history under constant amplitude loading is shown in Fig. 5. The stress range S_r and the number of cycles to failure N_f are often used to characterise the result of a constant amplitude fatigue test. A typical experimental study of constant amplitude fatigue for a certain design and material entails significant trials. Test results are often shown as

an S-N curve, with the stress range on the ordinate and the number of cycles on the abscissa, as shown in Fig.6.

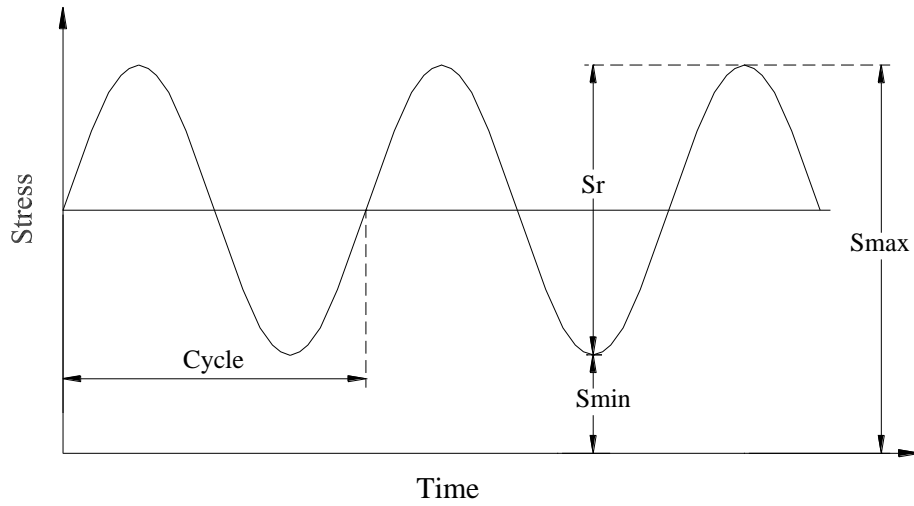


Fig. 5. An illustration of a stress history under constant amplitude loading.

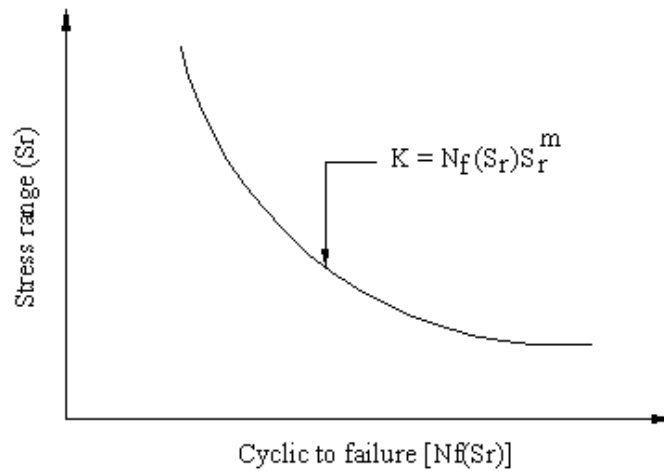


Fig. 6. A typical S-N curve for outcomes of constant amplitude experiments.

The S-N curve, to characterize concrete fatigue is expressed by results from laboratory tests from several sources is given by

$$N_f = K S_r^{-m} \tag{4}$$

Where, K, m = positive material constants whose values vary depending on the material and geometry of the specimen;

S_r = stress range;

N_f = number of cycles to failure denoted;

7.2. Damage accumulation hypothesis

In practise, however, a vehicle going over a pavement causes dynamic load due to vehicle oscillation produced by pavement roughness. Because of the random nature of the pavement roughness, these load time histories are much more complicated than periodic loadings employed in laboratory fatigue testing. The load-time history is typically dominated by one major cycle equivalent to the vehicle's peak live load. Dynamic effects produce extra little cycles on top of the large cycle. To estimate the fatigue damage induced by vehicle passing, both the large dominant cycle and the small-superimposed cycles must be considered. The fundamental objective of fatigue analysis is to utilise the S-N curve data from periodic testing to forecast the fatigue life of an element or assembly exposed to a service load with a complex time history. Without further information, Eq. (4) cannot be employed in the situation of random load history. Cumulative damage rules are often used to account for the influence of variable-amplitude loading (i.e., random load or irregular) on fatigue performance. These principles often seek to match fatigue behaviour with a complicated loading history to known behaviour with constant amplitude loading. The linear damage accumulation concept, often known as the "Palmgren-Miner" hypothesis [19], was applied in this work. Under variable-amplitude loading, the cumulative damage buildup is given by

$$D(t) = \sum_{j=1}^{n_b} \Delta D_j = \sum_{j=1}^{n_b} \frac{n_j}{N_j} \quad (n_j \leq N_j) \quad (5)$$

where D_j is the incremental damage, n_j is the number of stress cycles at stress range level S_{rj} , N_j is the number of cycles at constant stress range level S_{rj} from the (S-N curve) to induce failure, and n_b is the number of stress range blocks in the histogram. The fatigue life T is then calculated as $T=1/D(t)$. Using S-N curve relation in Eq. (5), the damage function at $t=T$ can be written as

$$D(t) = \sum_{j=1}^{N(T)} \frac{n_j}{K S_r^{-m}} = K^{-1} \sum n_j S_r^m \quad (6)$$

The Palmgren-Miner rule has a severe disadvantage in that it does not account for sequence effects, which means that the order of the loading makes no difference even though their impacts are clearly detected in many circumstances.

7. 3. Approach for fatigue life predication

Several ways to fatigue prediction exist, each with a different level of stress and strain analysis. Vibrations in the airfield pavement are caused by moving vehicles. The ensuing oscillating strains cause damage to accumulate in the pavement components over time. The current study includes fatigue damage estimations for the pavement based on vehicle produced stress history and fatigue strength values obtained from standards. The time domain analysis utilising simulated response time history- Cycle counting approaches were utilised in the first approach to determine cycle range and then to create the stress range frequency histogram while taking yearly traffic volume into account. The linear damage accumulation theory is used to determine fatigue life by

determining the number of cycles per year that correspond to a certain stress range and the number of cycles that may be sustained at that stress range before fatigue failure.

7.3.1. Rainfall cycle counting method

Cycle counting has been defined as a method for converting a loading time history into a number of cycles. There are many several counting approaches for classifying random time histories [20]. The Rain-flow Counting Approach (RFCM) was employed in the time domain cycle counting method in the current investigation to define cycle range. This approach produces a one-to-one relationship between the stress time history's local maxima and minima. Small cycles in RFCM are seen to be interruptions of larger cycles. The approach suggests both slowly variable high amplitude cycles and more fast small reversals on the top or bottom of these cycles in this way. Appendix C illustrates the sequence of operations used in the RFCM approach. In practise, the rain-flow technique of cycle counting is extensively utilised.

The Rain-flow Approach may detect occurrences in a complex stress sequence that are compatible with constant-amplitude fatigue data and Low frequency stress range cycles. The essential principle underlying any stress cycle identification system is to define a half cycle to be the section of a stress time history $\sigma_r(x,t)$ between any two successive local extremes (from peak to valley or valley to peak). The stress-time history is used to evaluate random processes in relation to structural fatigue. The rain-flow counting approach is based on the basic assumption that fatigue damage caused by small induced stress cycles may be added to fatigue damage caused by big stress cycles. According to Fig.7, it can be seen that if the cycle 1–4 is interrupted by a small cycle 2–3–2', the coordinate of the point 2' is very near to the point 2 and the material acts as if no interruption by an inserted cycle has taken place. Moreover, one complete cycle 2–3–2' has remained at disposal.

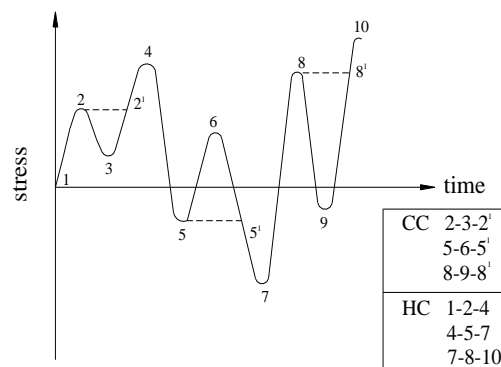


Fig.7. Stress-time history (CC-Complete Cycles, HC-Half Cycles).

8. Results and discussion

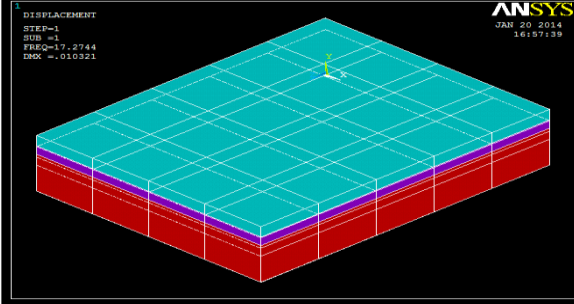
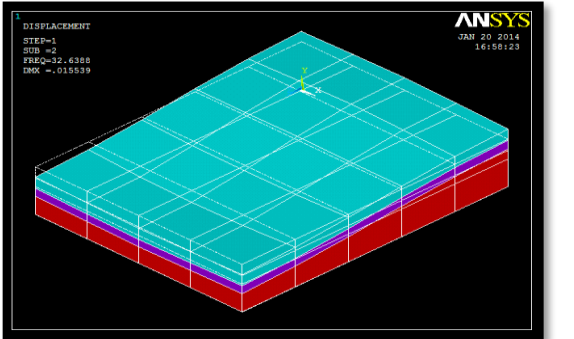
The dynamic (transient) analysis of the existing and the proposed runway is carried out for the parameters such as take-off speeds of 160 kmph and 260 kmph corresponding to A-310 and A-380. In this study compare the aircraft's dynamic effects on two concrete types belonging to conventional or standard strength and high strength concrete.

8.1. Modal analysis

The modal parameters of pavement model like the natural frequencies and mode shapes have been evaluated using the adopted finite element model for study. Mainly, the effect of thickness and Elastic Modulus of concrete pavement on the free vibration characteristics of pavement has been studied. The mass density of the bridge materials is 2403 kg/m^3 , while modulus of elasticity and Poisson's ratios has been taken as $3.0 \text{ e}+10 \text{ N/m}^2$ and 0.15. First six frequencies and mode shapes have been presented in Table 2 for the pavement with the thickness of 20 cm. The evaluation of natural frequencies and mode shapes have also been carried out corresponding to a finite element representation using the conventional 8noded Solid element having six degrees of freedom only and have been presented in Table 2. Further, in order to demonstrate the effect of thickness of pavement on the free-vibration, analyses have been carried out with varying thickness (20 cm – 40 cm) of the pavement. Table 3 shows the variation of frequencies of the bridge with the change in the thickness and Elastic Modulus of the pavement. The Table shows that the frequencies change slightly with the increase in the thickness and Elastic Modulus of pavement.

Table 2

Mode shape for airfield pavement considering 6 d.o.f elements.

Mode	Natural Frequencies (Hz)	Cyclic Frequencies (Hz)	Time Period (sec)	Mode Shape
1	17.2744	1.374	0.3635	
2	32.6388	5.1947	0.1924	

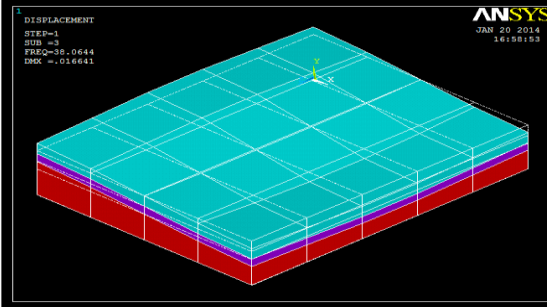
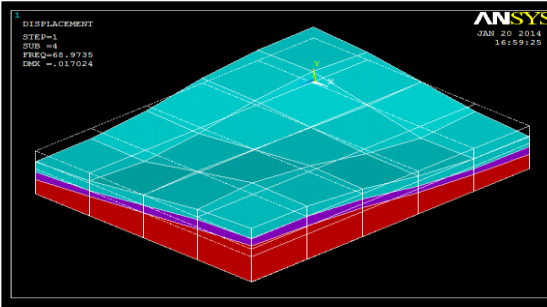
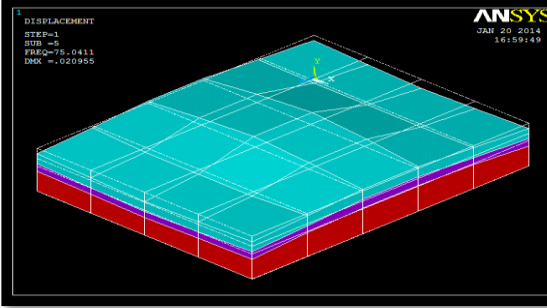
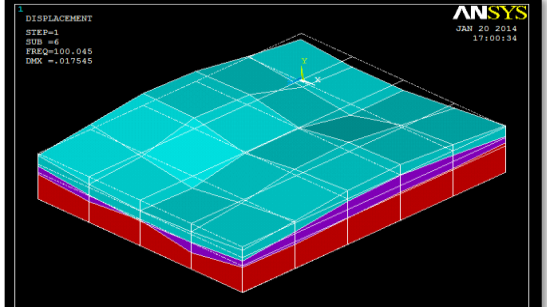
3	38.0644	6.0581	0.1649	 <p>DISPLACEMENT STEP=1 SUB =3 FREQ=38.0644 DOF =.016681</p> <p>ANSYS JAN 20 2014 16:58:53</p>
4	68.9735	10.9774	0.0910	 <p>DISPLACEMENT STEP=1 SUB =4 FREQ=68.9735 DOF =.017024</p> <p>ANSYS JAN 20 2014 16:59:25</p>
5	79.0411	12.5797	0.07945	 <p>DISPLACEMENT STEP=1 SUB =5 FREQ=79.0411 DOF =.020955</p> <p>ANSYS JAN 20 2014 16:59:49</p>
6	100.045	15.9226	0.06277	 <p>DISPLACEMENT STEP=1 SUB =6 FREQ=100.045 DOF =.017545</p> <p>ANSYS JAN 20 2014 17:00:34</p>

Table 3Modal Analysis Results Showing Fundamental Natural Frequency ω in Hertz.

Elastic Modulus, E (MPa)	Mode Shape	Slab Thickness, h (cm)				
		20	25	30	35	40
30000	1	17.27	15.77	14.61	13.67	12.89
	2	32.63	32.63	32.76	32.99	33.32
	3	38.06	38.44	38.90	39.45	40.08
	4	68.97	70.59	72.08	73.54	74.99
	5	75.04	77.32	79.44	81.53	83.62
	6	100.04	100.04	100.04	100.04	100.04
40000	1	17.24	15.75	14.59	13.65	12.87
	2	38.98	39.36	39.82	40.34	40.92
	3	46.19	47.01	47.85	48.74	49.67
	4	85.72	88.03	90.09	92.061	93.99
	5	93.34	77.31	99.27	102.01	104.72
	6	100.04	100.04	100.04	133.64	133.69

8.2. Calculation of fundamental time period and time steps

The time step is the most important aspect in transient movement analysis since it impacts the accuracy of the results. Time steps by calculation are found for each pavement thicknesses, which is illustrated below (Table.4).

Table 4

Calculation of Fundamental Time Period.

Fundamental time period(T)= $2\pi/\omega=2*3.14/17.274$
Elemental traverse time(ΔT)= $(1/50) \times$ Fundamental time period(T)= $0.394813/50$
Elemental length(ΔL)= $\Delta T * V=(0.007896*260*1000)/(60*60)=0.6$
Number of load steps= Slab length (L) / elemental length (ΔL)= $4.5/0.6 = 8$

As a result of manual calculation the time step in seconds is found to be 0.007, 0.00865, 0.00934, 0.00998, 0.01058 for pavement thicknesses of 20 cm, 25 cm, 30 cm, 35cm, 40cm.

8.3. Determination of stress time history curve by dynamic analysis

The distribution of load between the landing gears and between the wheels of landing gear is considered to be uniform. The dynamic loading type chosen is of ramped type as it simulates the gradual loading and un-loading by the aircraft wheel load. The element length is obtained as a result of manual calculation and the time step between successive loadings is found out. The time steps for various pavement thicknesses of 20 cm, 25 cm, 30 cm, 35cm, and 40cm were 0.007sec, 0.00865sec, 0.00934 sec, 0.00998 sec, 0.01058sec respectively. Using these time steps the elemental length i.e. node to node distance for each traverse of the landing gear's wheel load is determined. This segmentation is done as per the requirement of clarity in graphical representation of stress points. The dynamic - transient analysis for wheel loads is carried out by varying the

location TRDT and TADT wheel loads along the pavement edge for these time steps on each pavement thicknesses of 20 cm, 25 cm, 30 cm, 35 cm, and 40 cm, moving at take-off speeds of 160 kmph and 260 kmph along the edge of the pavement. The final comparison is brought out between the conventional and high strength concrete. The result of the space varying aircraft wheel's ramped loading is the stress-time history graphs, which shows the time in seconds and stress in kg/cm^2 along the x and y axis respectively. The stress-time history graphs shown in Fig.8 to 11 for a specific node point, preferably at the midway of the edge of the slab is considered, as it yields the most critical stress values. The interval between subsequent time steps for dynamic wheel loading is segmented into 10 number of sub-steps. Major deductions such as the maximum time varying stress resultants from the stress history curves could be inferred. The maximum range of resonating dynamic stress for aircraft take-off speed of 160 kmph on both the concrete types is found to be $\pm 3\text{kg}/\text{cm}^2$, which for the speed category of 260 kmph is found to be around $\pm 4\text{kg}/\text{cm}^2$.

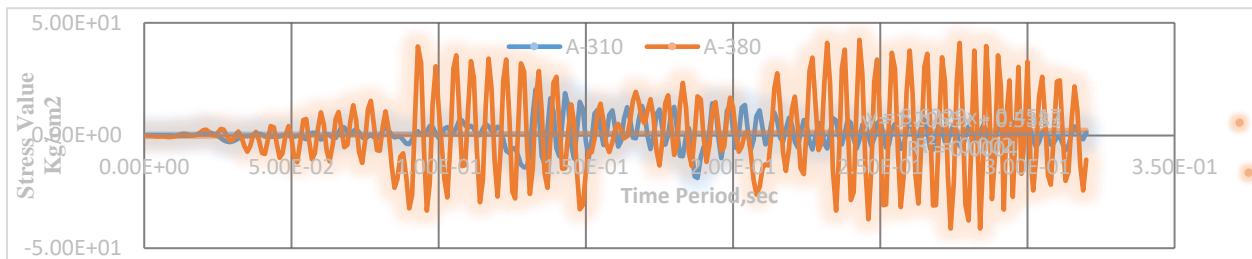


Fig. 8. Stress-Time History Curve for Speed= 160 kmph, h=20cm, E=30000MPa.

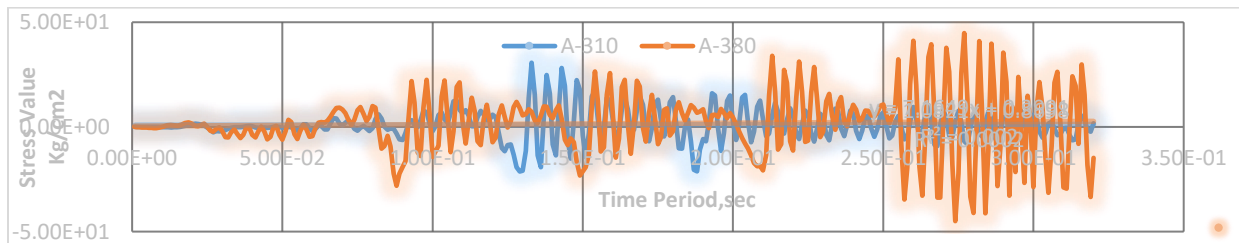


Fig. 9. Stress-Time History Curve for Speed =160 kmph, h=20cm, E=40000MPa.

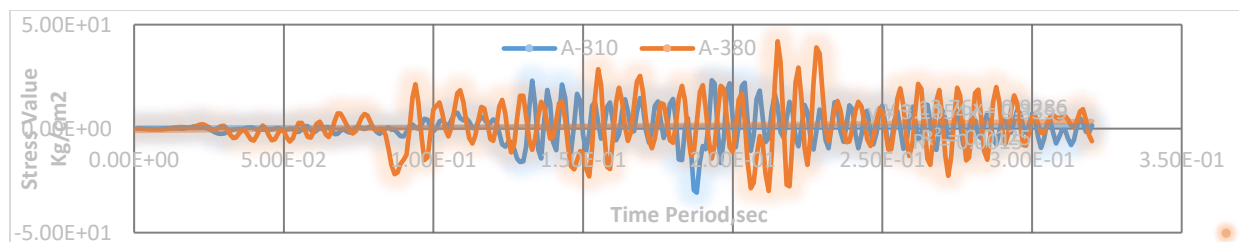


Fig. 10. Stress-Time History Curve for Speed = 160 kmph, h=25cm, E=30000MPa.

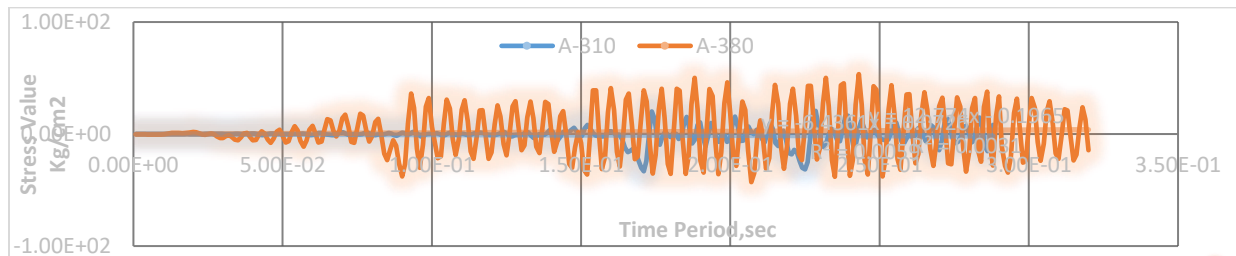


Fig. 11. Stress-Time History Curve for Speed = 160 kmph, h=25cm, E=40000MPa.

8.4. Evaluation of fatigue life by Miner's rule and RFCM

Fig. 12 to Fig.13 shows the dynamic (transient) stress time history graph which is fed into RFCM algorithm, which on further manipulation gives the fatigue life of the pavement. The stress histogram after repeating the time history curve using the Rain flow counting technique for the flexural stress specimens by simulation at the mid-length of the pavement. It should be mentioned that the flexural stresses were calculated using the landing gear of a single aircraft vehicle crossing the pavement. Table 5 shows the fatigue life of pavement in years which varies from 17.29 to 73.57 for A-380 having take-off speed of 260kmph. For A-310 bearing TADT having take-off speed of 260kmph the fatigue life is found to vary from 10.96 to 46.65years. The above inference is taken for two concrete types namely, conventional or standard strength concrete and high strength concrete. It also shows that the fatigue life increases with slab thickness as well as the predefined concrete strength. Though the A-380 has greater gross weight than A-310, its fatigue life is found to be higher. This goes by the fact that a material's fatigue property purely depends on the load frequency rather than its magnitude. The variance in fatigue life value for A-380 and A-310 with take-off Speed of 160kmph is found to vary from the results of 260 kmph by only a negligible amount. The damage index of the pre-mentioned concrete types and pavement thickness i.e., the ratio of fatigue life consumed is also tabulated. Since these values are within the allowable limits i.e., 1 (limiting factor specified by Miner's rule), it makes the pavement structure to be within the safe limits and fit for future usage. But due considerations is to be given as in the case of number of fatigue years as it would make significant difference. Table 4 also shows the total number of half and full cycles which are resultant of the RFCM programmed using MATLAB tool. Assuming constant traffic throughout the year, the number of cycles obtained from Rainflow analysis is easily transformed into annual cycles by employing a constant multiplier (essential or design aircraft's annual departure number). The yearly flow rates of all aircrafts over the runway are 5331 and 3507 in terms of A-310 and A-380. Figures 15 and 16 illustrate a typical stress range vs. frequency (number of cycles/year) histogram for two aircrafts with forward speeds of 160km/hr and 260km/hr and sprung masses of 67kN and 165kN, respectively. The Airfield Pavement is determined to be exposed to a maximum of 4 10⁷ to 6 10⁷ cycles per year in the stress range of 0.0657 kg/cm²-0.1064 kg/cm² (mean stress 0.086 kg/cm²) at operating aircraft vehicle speeds of 160km/hr and 260km/hr. The number of stress cycles encountered by the Airfield Pavement seems to decrease in the higher stress range.

Table 5

Fatigue life and Damage index for A-310 and A-380 having Take-Off Speed of 260 kmph.

Aircraft		Elastic Modulus, MPa	30000				40000			
Speed	Type	thickness, cm	Full cycle	half cycle	Fatigue life, Years	Damage Index	Full cycle	half cycle	Fatigue life, Years	Damage Index
260 kmph	A-310	20	152	4	10.9564	0.0913	117	0	23.3231	0.0429
		25	257	0	13.7091	0.0729	127	0	29.1539	0.0343
		30	127	0	16.4509	0.0608	126	0	34.9846	0.0286
		35	96	0	19.1927	0.0521	96	0	40.8154	0.0245
		40	125	0	21.9346	0.0456	96	0	46.6462	0.0214
	A-380	20	156	0	17.2968	0.0578	154	2	36.7836	0.0272
		25	156	0	21.6210	0.0463	156	0	45.9795	0.0217
		30	155	1	25.9453	0.0385	155	0	55.1754	0.0181
		35	116	0	30.2695	0.0330	116	0	64.3713	0.0155
		40	117	0	34.5937	0.0289	116	0	73.5672	0.0136

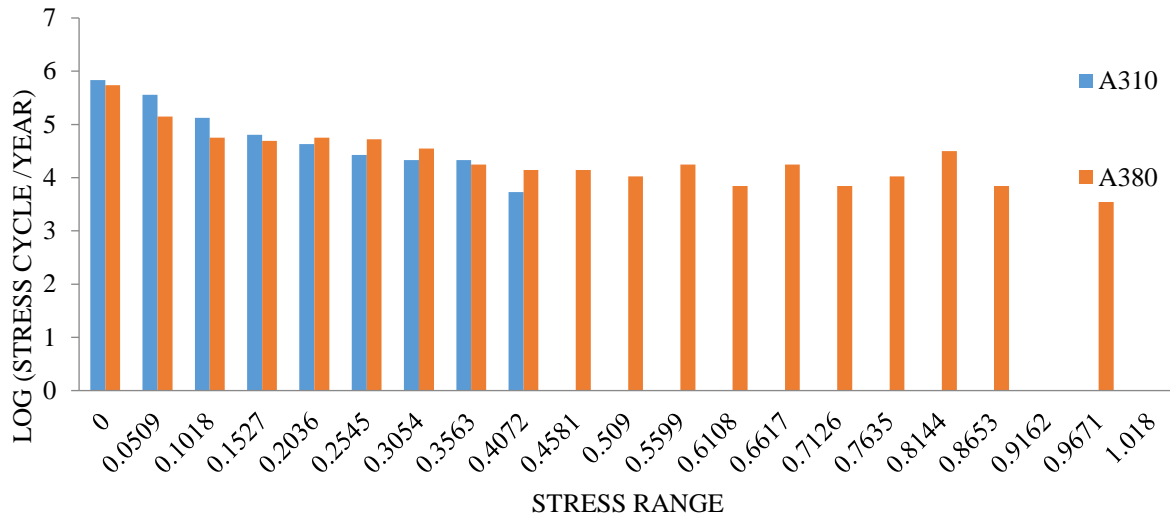


Fig. 12. Histogram for Stress ranges vs. Frequency (cycles/year) for A-310 and A-380 (h=20cm,E=30000MPa).

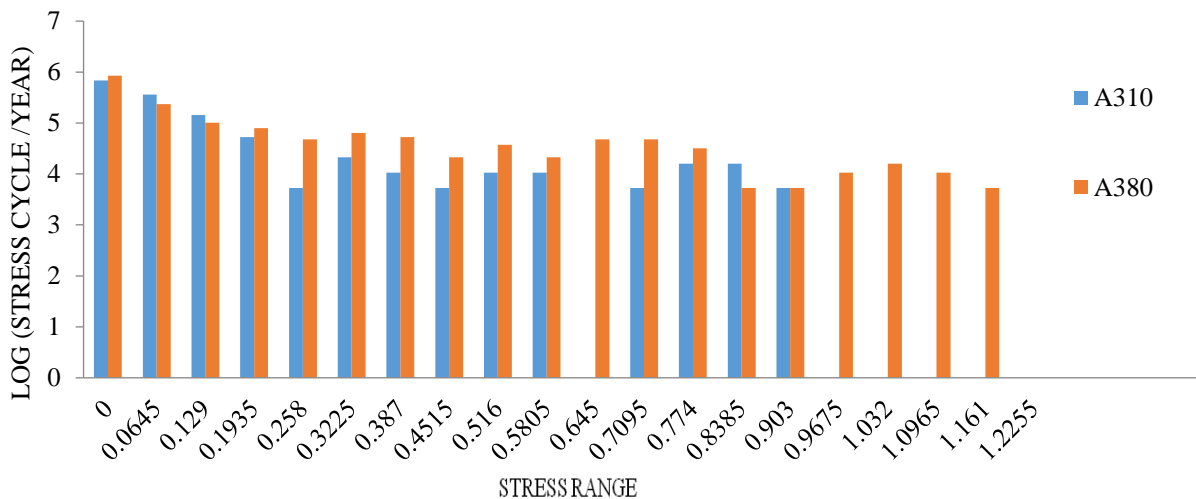


Fig. 13. Histogram for Stress ranges vs. Frequency (cycles/year) A-310 and A-380 (h=25cm,E=40000MPa).

9. Conclusions

A computationally efficient finite element has been used to model airfield pavement which takes into account the usual extensional, flexural and torsional behavior. The applicability of such an element for the dynamic analysis has been verified by evaluating the modal parameters of an airfield pavement model theoretically. The dynamic response of pavement due to moving airfield vehicle has been studied considering speed of the vehicle. Another important feature of the present study is the estimate of fatigue life through the application of linear damage accumulation rule. The time domain cycle counting method yields the stress histogram from which fatigue life has been evaluated. The rainfall counting method has defined a systematic technique for calculating

the fatigue life of rigid airport pavement while taking into account its dynamic interaction with aircraft wheel load. The parametric study indicates that proper maintenance and periodic inspection is necessary to reduce the tendency of fatigue failure in the pavement component. The study also focused on finding the structural capability for the extended runway by carry out dynamic and fatigue analysis. This section discusses the various conclusions on the study project.

The major observations from the present study may be summarized as follows:

1. A computationally less expensive and realistic 3-D element with 8 noded -Solid 185 element type has been utilized for the modeling of the pavement. The applicability of such an element for the dynamic analysis has been verified by evaluating the modal parameters of a pavement theoretically.
2. Free vibration studies of airfield pavement show that the natural frequencies of pavement little decrease with the increase of thickness of pavement.
3. The fatigue life of the pavement is dependent on the airfield vehicle wheel load, and the speed of the airfield vehicle, thickness and Elastic Modulus of concrete pavement.
4. The fatigue life of the bridge increases with the increase of airfield pavement slab thickness.
5. The fatigue life of the bridge increases with the increase of airfield pavement concrete strength by Elastic Modulus. The inherent property of strain increment with decrease in elastic property of concrete was found to be comprehensive as the variation in fatigue life was found to be around 50 % higher when high strength concrete was used rather than conventional or standard strength concrete. Moreover the variation was found to be 36 % higher for A-310, inspite of A-380's heavier gross weight. Thus the inherent property of strain increment with decrease in elastic property of concrete was found to be comprehensive by this fatigue analysis.
6. The damage accumulation progresses rapidly due to increase of the vehicle load, decreasing the fatigue life. The variance in fatigue life value for A-380 and A-310 with take-off Speed of 160kmph is found to vary from the results of 260 kmph by only a negligible amount.

The integrated module has been developed involving analysis of airfield pavement using a computationally efficient finite element, assessing the safety limit of the pavement by evaluating fatigue life. This module could be used for many important observations critical to efficient design of the airfield pavement.

Funding

This research received no external funding.

Conflicts of interest

The authors declare no conflict of interest.

References

- [1] Kukreti AR, Taheri MR, Ledesma RH. Dynamic Analysis of Rigid Airport Pavements with Discontinuities. *J Transp Eng* 1992;118:341–60. [https://doi.org/10.1061/\(ASCE\)0733-947X\(1992\)118:3\(341\)](https://doi.org/10.1061/(ASCE)0733-947X(1992)118:3(341)).
- [2] Taheri MR, Zaman MM. Effects of a moving aircraft and temperature differential on response of rigid pavements. *Comput Struct* 1995;57:503–11. [https://doi.org/10.1016/0045-7949\(94\)00625-D](https://doi.org/10.1016/0045-7949(94)00625-D).
- [3] Wu C-P, Shen P-A. Dynamic Analysis of Concrete Pavements Subjected to Moving Loads. *J Transp Eng* 1996;122:367–73. [https://doi.org/10.1061/\(ASCE\)0733-947X\(1996\)122:5\(367\)](https://doi.org/10.1061/(ASCE)0733-947X(1996)122:5(367)).
- [4] Rahman SO, Anam I. Dynamic analysis of concrete pavement under moving loads. *J Civ Environ Eng* 2005;1:1–6.
- [5] Shoukry SN, Fahmy M, Prucz J, William G. Validation of 3DFE Analysis of Rigid Pavement Dynamic Response to Moving Traffic and Nonlinear Temperature Gradient Effects. *Int J Geomech* 2007;7:16–24. [https://doi.org/10.1061/\(ASCE\)1532-3641\(2007\)7:1\(16\)](https://doi.org/10.1061/(ASCE)1532-3641(2007)7:1(16)).
- [6] Sawant V. Dynamic analysis of rigid pavement with vehicle–pavement interaction. *Int J Pavement Eng* 2009;10:63–72. <https://doi.org/10.1080/10298430802342716>.
- [7] Zhong Y, Gao Y, L. M. Dynamic Response of Rigid Pavement Under Moving Traffic Load With Variable Velocity. *Balt J Road Bridg Eng* 2012;7:48–52.
- [8] Patil VA, Sawant VA, Deb K. 2-D finite element analysis of rigid pavement considering dynamic vehicle–pavement interaction effects. *Appl Math Model* 2013;37:1282–94. <https://doi.org/10.1016/j.apm.2012.03.034>.
- [9] Shafabakhsh G. Analysis of runway pavement response under aircraft moving load by FEM Gholamali Shafabakhsh, Ehsan Kashi, Mojtaba Tahani n.d.
- [10] Li ZX, Chan THT, Ko JM. Fatigue damage model for bridge under traffic loading: application made to Tsing Ma Bridge. *Theor Appl Fract Mech* 2001;35:81–91. [https://doi.org/10.1016/S0167-8442\(00\)00051-3](https://doi.org/10.1016/S0167-8442(00)00051-3).
- [11] Roesler JR. Fatigue resistance of concrete pavements. 6th Int. DUT–Workshop Fundam. Model. Des. Perform. Concr. Pavements, 2006.
- [12] Leander J, Karoumi R. Dynamics of thick bridge beams and its influence on fatigue life predictions. *J Constr Steel Res* 2013;89:262–71. <https://doi.org/10.1016/j.jcsr.2013.07.012>.
- [13] R D, Piotr. Effect of pavement roughness and vehicle dynamic loads on decrease of fatigue life of flexible pavements. *Proc 7th Transp Res Arena* 2018:16–9.
- [14] Liu C, McCullough BF, Oey HS. Response of Rigid Pavements due to Vehicle-Road Interaction. *J Transp Eng* 2000;126:237–42. [https://doi.org/10.1061/\(ASCE\)0733-947X\(2000\)126:3\(237\)](https://doi.org/10.1061/(ASCE)0733-947X(2000)126:3(237)).
- [15] Wu C, Wang H, Zhao J, Jiang X, Yanjun Q, Yusupov B. Prediction of Viscoelastic Pavement Responses under Moving Load and Nonuniform Tire Contact Stresses Using 2.5-D Finite Element Method. *Math Probl Eng* 2020;2020:1–16. <https://doi.org/10.1155/2020/1029089>.
- [16] Yuan J, Li W, Li Y, Ma L, Zhang J. Fatigue Models for Airfield Concrete Pavement: Literature Review and Discussion. *Materials (Basel)* 2021;14:6579. <https://doi.org/10.3390/ma14216579>.
- [17] Rahmawati A, Rahmawati F. Runway Pavement Strength Evaluation of Yogyakarta International Airports Depends on ICAO (ACN/PCN) Method with COMFAA 3.0 Software. *Int J Integr Eng* 2022;14:350–9.
- [18] White G. Difference between Pavement Thickness Design and Pavement Life Prediction for Rigid Aircraft Pavements. *Designs* 2022;6:12.
- [19] Lutes LD, Sarkani S. Stochastic analysis of structural and mechanical vibrations. Prentice Hall; 1997.
- [20] Ladislav F. Dynamics of railway bridges 1996.

Appendix-A

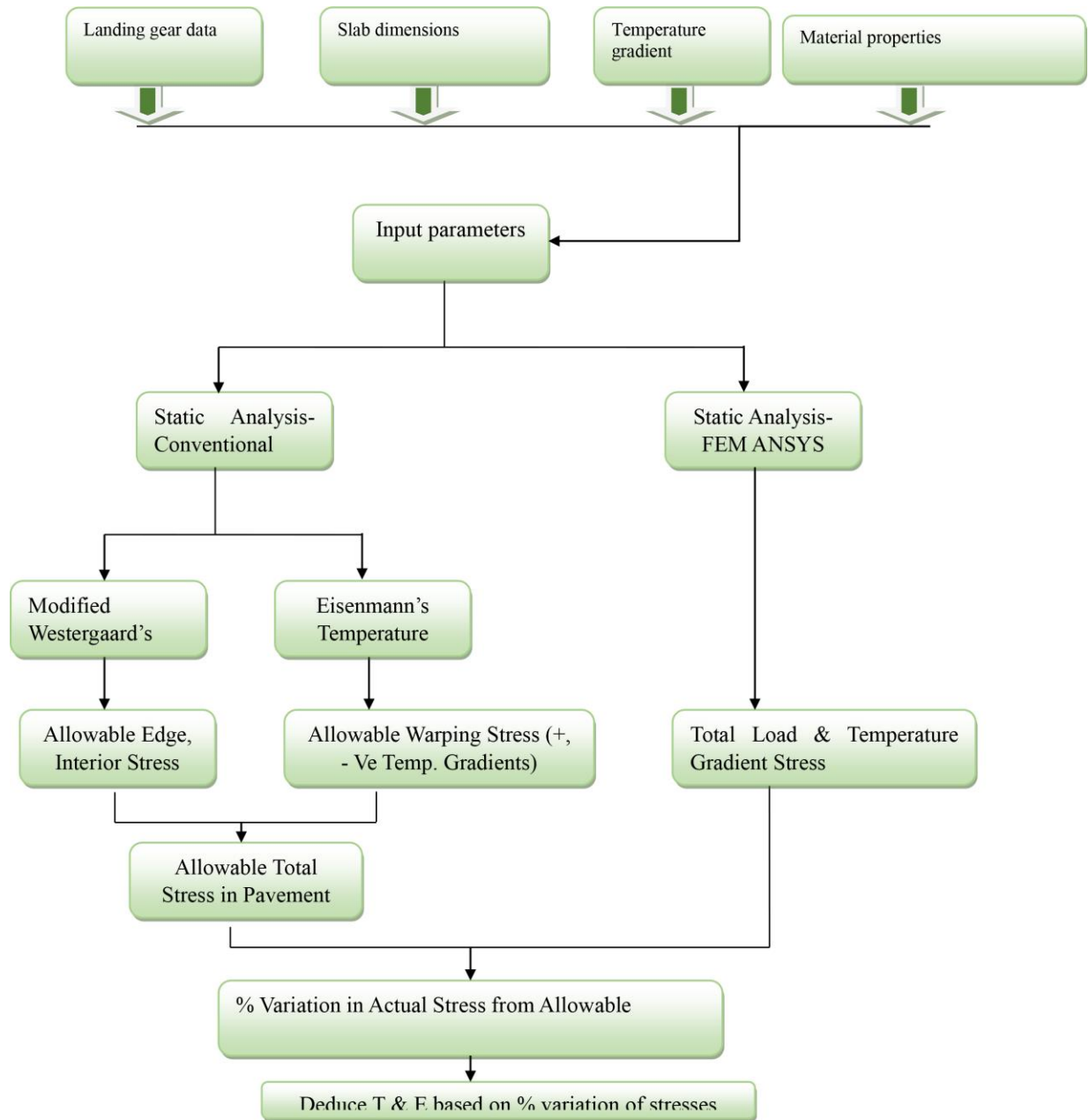


Fig .14. Deduction of thickness and Modulus of Elasticity using conventional and FEM (ANSYS) for static loads

Appendix-B

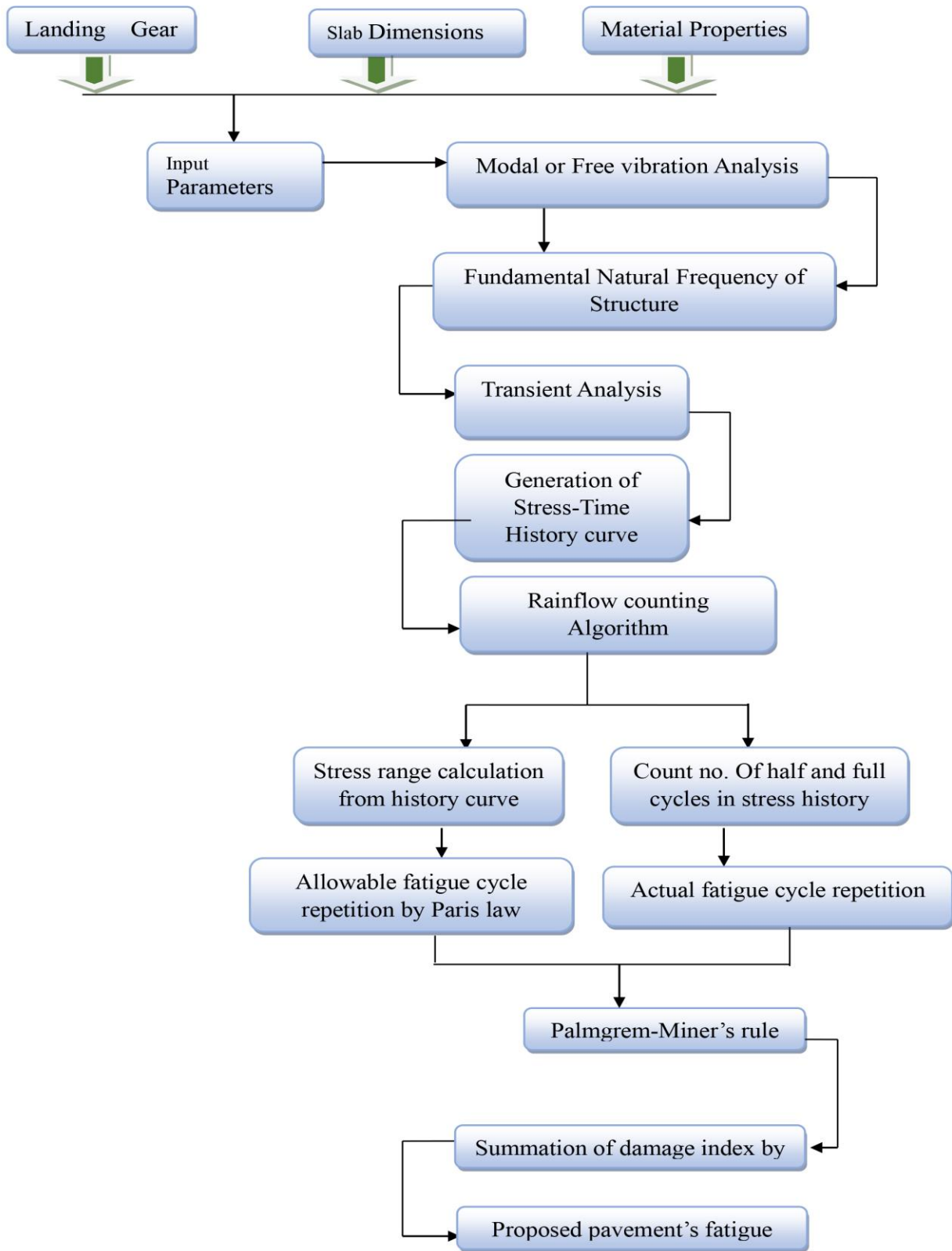


Fig.15. Fatigue life of proposed runway using dynamic analysis

Appendix-C

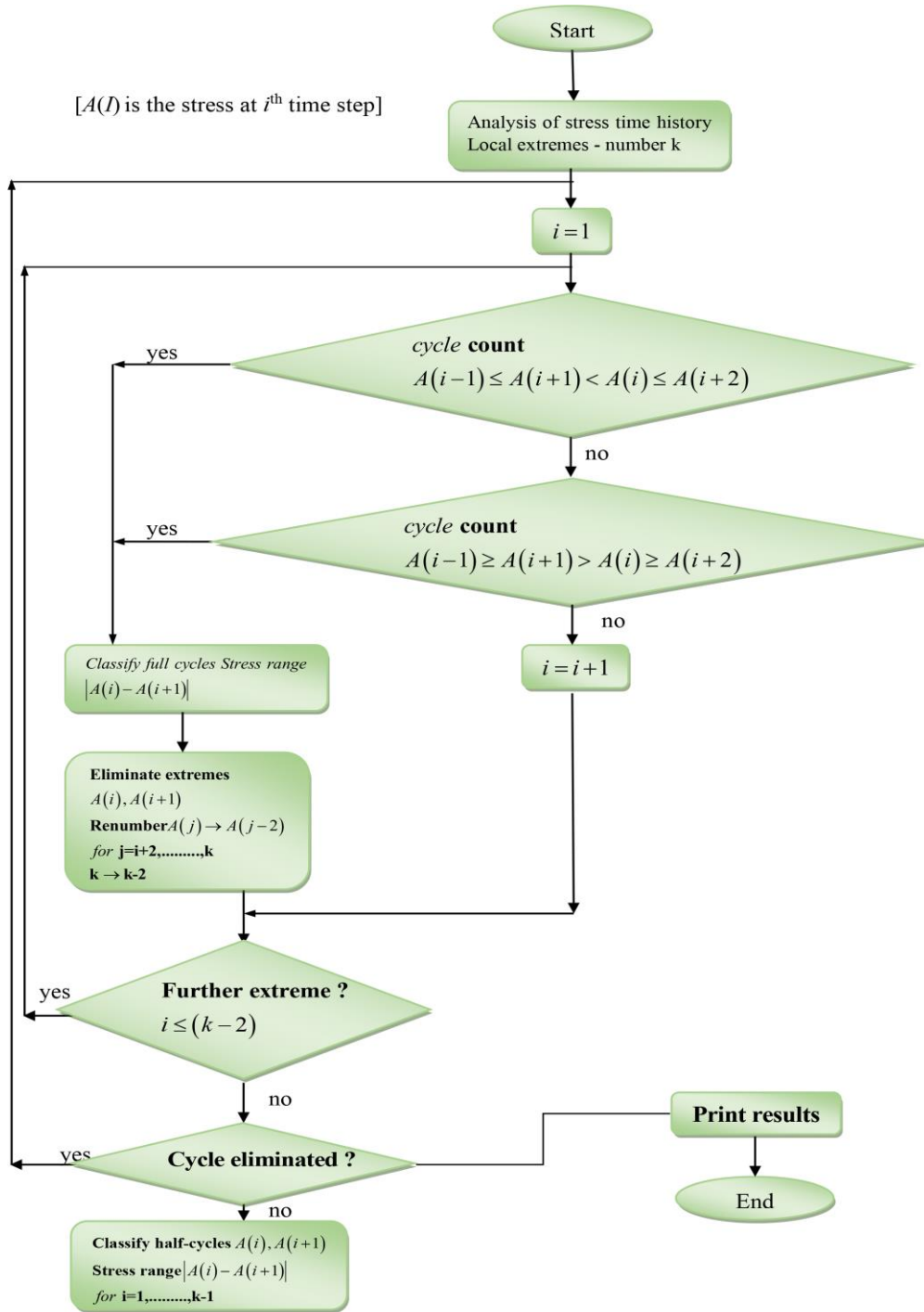


Fig .16 Fatigue life of proposed runway using dynamic analysis